Special Issue of the International Conference on Research and Applications of Plasmas (PLASMA-2019)

Stark-Broadening Studies of N(I) Multiplet $3p\ ^4P^o$–$3d\ ^4D$ at 1052.630 nm

A. Bartecka*, A. Bacławski and W. Olchawa

Institute of Physics, University of Opole, Oleska 48, 45-052 Opole, Poland

Doi: 10.12693/APhysPolA.138.650 *e-mail: bartecka@uni.opole.pl

Stark-broadening studies of the N(I) multiplet $3p\ ^4P^o$–$3d\ ^4D$ are reported. Our experimental electron impact widths of spectral lines are compared with the results of our calculations: (i) according to the standard impact theory of Griem with modification, (ii) using a computer simulation method which is based on numerical N-body code (CSM). Line shape measurements were performed using a wall-stabilized arc. The radiation of the plasma emitted from homogenous plasma layers was measured using a grating spectrometer equipped with a two-dimensional detector.

topics: Stark broadening, line shapes, optical measurements, computer simulations

1. Introduction

Investigations of the Stark broadening of spectral lines emitted by atoms are useful for laboratory plasma diagnostics, because they provide information concerning one of the main parameters of plasma — electron density, N_e. In particular, when the Stark effect dominates over other broadening mechanisms for a given spectral line, the electron density of plasma can be deduced from non-hydrogen line widths [1, 2] which exhibit linear dependence on N_e. The widths of non-hydrogenic lines in the visible and infrared part of the spectrum are usually significantly smaller in comparison to the widths of hydrogen Balmer lines, commonly used for electron density determination. However, data on the widths of the non-hydrogenic lines are important for studies of plasmas, where hydrogen is not present or is undesirable.

Indeed, for example, spectral lines of nitrogen, due to rather large abundances of nitrogen in stars, can also have application in astrophysical plasmas investigations, especially in investigations of abundances of light elements in astrophysical objects and in the analysis and modeling of the radiation transport in stellar atmospheres.

In this work, we determined the experimental electron impact widths w_e of lines belonging to the investigated multiplet. Stark broadening studies of the infrared N(I) $3p\ ^4P^o$–$3d\ ^4D$ multiplet are reported for the first time. The experimental results are compared with the results of our calculations, performed according to the impact theory of Griem [3] with modification [4, 5] and with our results of the computer simulation method (CSM) [5, 6].

We also tested the CSM which extends the range of applicability of computer simulations, mainly used for hydrogen, hydrogen-like and helium lines. The w_e values obtained by the CSM agree with the experimental ones satisfactorily.

2. Experiment

Line shape measurements were performed using a high current wall-stabilized arc running in helium (86% by volume) and argon (10%) with small admixtures of nitrogen (2.4%) and hydrogen (1.6%) under atmospheric pressure. The scheme of the arc construction is presented in Fig. 1. The stabilizing wall consists of several copper plates isolated from each other by the insulator spacers and forms a discharge channel of a length of 80 mm and diameter of 4 mm. At both ends of this channel, two carbon cylindrical drilled through electrodes were mounted. A detailed description of the arc source and operation conditions can be found in [7, 8].

The concentration of nitrogen in the plasma was kept at a rather small level in order to avoid possible self-absorption of N(I) lines radiation along the arc axis. The areas close to the electrodes were additionally supplied with some amount of argon in order to improve the stability of the discharge. Since our measurements were performed in an end-on direction, the presence of argon in the vicinity of electrodes also reduced significantly the contribution of N(I) and H radiation from cooler plasma layers as well as assured optically thin conditions for radiation originating from the central region of the arc column.

The arc was operated at five arc currents from 20 to 54 A in order to obtain different plasma parameters: electron densities and temperatures.

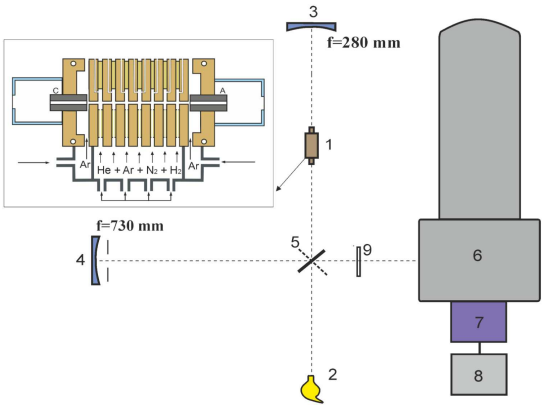

Fig. 1. The scheme of the experimental setup is shown: 1 — wall-stabilized arc, 2 — radiometric standard source, 3 and 4 — concave mirrors, 5 — swivel plane mirror, 6 — Ebert-type grating spectrometer, 7 — CCD detector, 8 — computer, 9 — spectral filter. In the left upper corner the scheme of the plasma arc (1) is presented.

The scheme of the experimental setup is presented in Fig. 1. The radiation emitted from thin plasma layers was measured in the end-on direction. The radiation originating either from the arc (1) or from the tungsten intensity standard lamp (2) was imaged via the flat rotational mirror (5) and the concave mirror (4) onto the 20 μm-wide entrance slit of the Ebert-type grating spectrometer PGS-2 (6) equipped with a grating with 1300 grooves/mm. The large focal length (730 mm) of the mirror (4) and the use of a diaphragm (12 mm) restrict the collection angle for the light emitted from the arc column and thus allow to select radiation originating from plasma layers parallel to the arc axis. The concave mirror (3) was applied for checking optically thin conditions of plasma layers parallel to the arc axis. In front of the entrance slit, a suitable edge filter (9) was placed in order to suppress the radiation from higher order spectra. The two-dimensional CCD detector (7) with regular pixel gaps of 0.026 mm was mounted in the exit focal plane of the spectrometer. This instrumentation provides spectra with a reciprocal dispersion of 7 pm/pixel for the studied nitrogen multiplet.

The arc plasma reveals the cylindrical symmetry with weak radial electron density gradients close to the arc axis. In the case of end-on observations, the applied optical imaging system of satisfactorily high spatial resolution assures that radiation originating from well-defined plasma volumes of nearly homogeneous electron densities could be measured [9, 10].

Besides the arc radiation, the radiation of the tungsten strip standard lamp has been measured in all studied spectral intervals. In this way, the measured intensities originating from the arc source could be converted to absolute radiance units. The low-pressure Plücker tube filled with neon was used as a standard source for wavelength calibration of the measured spectra and in order to determine the apparatus profile. At the entrance slit of the spectrometer set to 20 μm, the apparatus profile has been found to be of Gaussian type with a full width at half maximum (FWHM) of 13 pm.

3. Diagnostics

The main parameter determining the Stark broadening of spectral lines is the electron density of the plasma. We determined N_e from measured Stark widths of the hydrogen H_β transition. An example of the measured spectrum of the H_β line is presented in Fig. 2. Knowing the Stark widths of H_β line, we applied the commonly used standard theoretical broadening results of Gigosos and Cardeñoso [11] which include the contribution to the observed line widths arising from ion dynamic effects. For different arc currents and selecting various plasma layers, we measured spectra emitted from nearly homogeneous volumes, corresponding to electron density values from 0.5×10^{22} m^{-3} to 1.8×10^{22} m^{-3}.

Apart from the half widths of H_β, we also measured the peak separation of H_β profiles (see Fig. 2). In this way we were able to test if the radiation originates from the homogeneous plasma layers. According to the literature, the ratio of the distance between the peaks and the FWHM should be equal to 0.36 in homogeneous plasma [12, 13]. Since we restricted our measurements to plasma layers being not too far from the arc axis (about 1 mm), where the weak parameters gradients are observed, the homogeneity requirements were well fulfilled.

The plasma temperature was determined applying the standard Boltzmann plot method and by measuring total line intensities of three spectral lines of neutral nitrogen with wavelengths (in nm) 1056.333, 1064.398, and 1065.304 and one whole

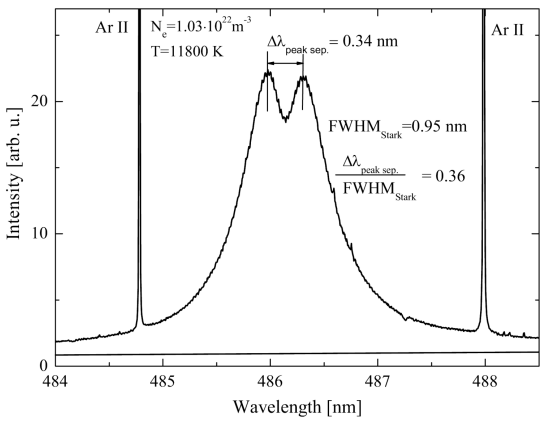

Fig. 2. The exemplary spectrum of the hydrogen H_β line used for electron density determination and plasma homogeneity verification.

nitrogen multiplet (1059.479 nm). Corresponding transition probabilities are 3.33×10^6 s^{-1}, 6.75×10^6 s^{-1}, and 9.03×10^6 s^{-1}, and for the N(I) multiplet 3.93×10^7 s^{-1}, respectively. The excitation energies of the chosen lines are in the range from 13.00 to 14.90 eV, i.e., the energy gap is sufficient for reliable temperature determination. The corresponding transition probabilities have been taken from [14, 15]. In this way — for different arc currents and plasma layers — temperatures in the interval from 8000 to 14000 K have been determined. The uncertainty of temperature determination has been estimated at about ±500 K. The accuracy of atomic constants, in particular the transition probabilities A_{ki}, has the greatest impact on uncertainty of temperature determination.

Assuming that the gas temperature is the same as the excitation temperature, it was possible to determine the Doppler broadening of spectral lines. For the studied nitrogen multiplet, the Doppler full width does not exceed 24 pm.

4. Fitting procedure

The N(I) $3p\ ^4P^o$–$3d\ ^4D$ multiplet consists of eight fine structure components. The spectra (after intensity and wavelength calibration against the standard sources) of the three spectral lines chosen for investigations at the following (non-shifted) wavelengths: 1053.38, 1053.96, and 1054.96 nm, which correspond to transitions between the levels with the following (lower-upper) J-values: 3/2-1/2, 5/2-7/2 and 5/2-5/2, respectively, at three different electron densities and plasma temperatures, are shown in Fig. 3.

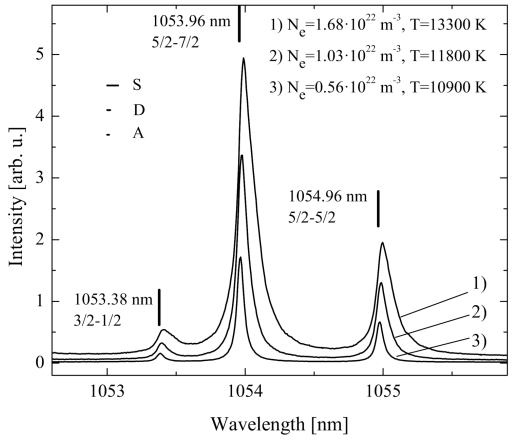

Fig. 3. The spectra of the chosen three lines of the N(I) $3p\ ^4P^o$–$3d\ ^4D$ multiplet at three different electron densities and plasma temperatures. The short vertical lines mark unperturbed wavelength positions. The horizontal lines illustrate (in the plot scale) Stark FWHM = 0.080 nm (S), Doppler FWHM= 0.022 nm (D) and apparatus FWHM = 0.013 nm (A) of the exemplary measured profile in plasma conditions 2).

Perpendicular lines mark the unperturbed wavelength positions of the lines. The broadening of the lines, increasing with higher electron density, is clearly visible. The lines are shifted relatively to the unperturbed wavelength positions and reveal considerable asymmetry. Broadening, shift, and asymmetry of the lines are associated mainly with the Stark effect. Horizontal lines, whose lengths mean the FWHMs of the Stark (S), Doppler (D) and instrumental profile (A) in the exemplary plasma conditions, allow to note that the Stark effect is the dominant broadening process in the case of our experiment.

To each measured spectrum (after radiance and wavelength calibration), taken from the given plasma layer of known electron density and temperature, the so-called profile of Griem [1] was fitted

$$j_{A,R}(\lambda) = j_{\max} \int_0^\infty \frac{W_R(\beta)\,\mathrm{d}\beta}{1 + \left[\frac{\lambda-\lambda_0-d_e}{w_e} - A^{4/3}\beta^2\right]^2}, \quad (1)$$

where $j_{\max}$ is the peak maximum, w_e is the electron impact width (HWHM), d_e — electron impact shift, $A = \left(C_4 F_0^2/e_0 w_e\right)^{3/4}$ — ion asymmetry parameter and $W_R(\beta)$ is the ion microfield distribution function at the neutral emitter position taken from [16]. The plasma screening parameter is denoted as $R = r_{0/}r_D$, $\beta = F/F_0$ is the reduced field strength (F_0 is the normal field strength depending on electron density), and C_4 is the constant of the quadratic Stark effect.

The double electron impact width of the spectral line is smaller than the full width at half maximum of this line. The relation between the FWHM, the electron impact width and the ion asymmetry parameter is written for neutral emitter in [1]:

$$\mathrm{FWHM} = 2\left[1 + 1.75A\left(1 - c_0 r\right)\right] w_e \quad (2)$$

with two dimensionless parameters: $c_0 = 0.75$ and $r \approx 9 \times 10^{-3} N_e^{1/6}/\sqrt{T}$. The electron density N_e is given in 10^{22} m^{-3}.

In the case of our experiment, we have to take into consideration additional broadening mechanisms, such us the instrumental and Doppler broadening. The shape of the instrumental profile as well as the Doppler one are described by Gaussian functions. The Griem-like profile is convoluted numerically with the appropriate Doppler and instrumental profiles. Finally, such a convoluted function is fitted to the experimental data. We have made an assumption that within a given multiplet, the widths and asymmetry parameters are the same for each fine structure component. We have also assumed the intensity ratio between fine structure components, taking into consideration transition probabilities from NIST database [14].

The fitting parameters are: the electron impact width and shifts of the lines, the ion asymmetry parameter, parameters of the background straight line and intensity of the strongest line.

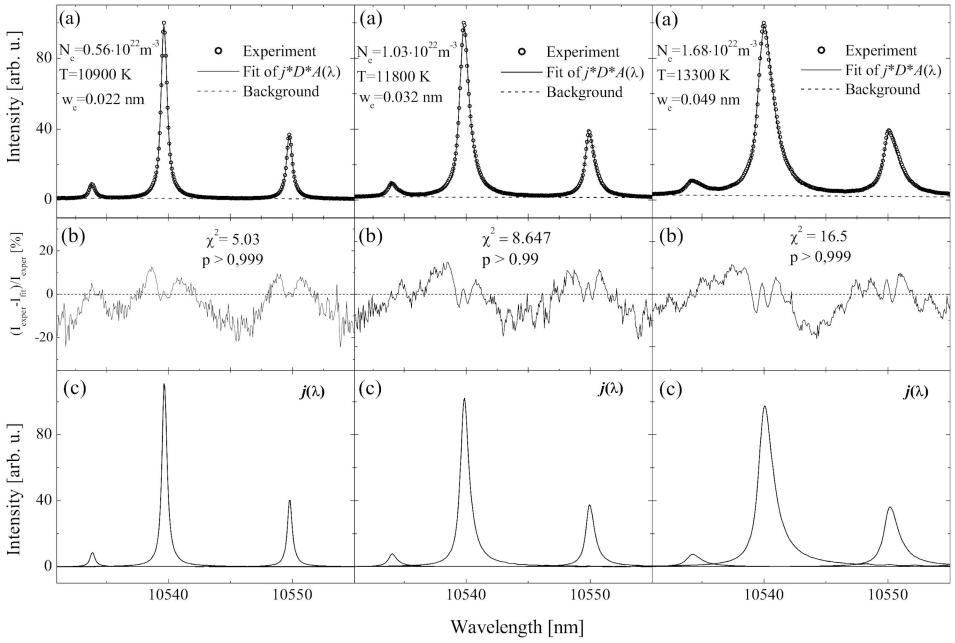

Fig. 4. The examples of the analysis of a measured spectrum (three chosen lines of the multiplet N(I) $3p\ ^4P^o$–$3d\ ^4D$), illustrating the fitting procedure in three different plasma conditions: (a) the comparison of measured spectrum (circles) and fitted function (solid line), the dashed line represents the background continuum, (b) the difference between the measured spectral intensity distribution and the fitted profile, (c) the pure Stark ($j\lambda$) profiles of the three fine structure components.

Examples of our measurements and the results of the final fitting procedure are shown for three different plasma conditions in Fig. 4. In the part of Fig. 4a, the experimental results are juxtaposed with the fitted sum of the $j\,(\lambda)$ profiles convoluted with appropriate Doppler and apparatus Gaussian functions. Residual plots representing the difference between the measured spectral intensity distribution and the fitted profiles are presented in Fig. 4b. As it can be observed, the difference does not exceed 10% at the line core. In Fig. 4c, the pure Stark broadened three fine structure components of the multiplet are shown.

5. Calculations

Apart from the fitting procedure, the calculations of the Stark broadening parameters of the investigated multiplet have also been carried out using two different methods.

The computations of $j(\lambda)$ profile are based on the impact approximation for electrons and quasi-static approximation for ions. We used Griem's theory and took into consideration the lower level perturbation [3]. The electron impact width and electron impact shift can be calculated in this case from

$$w_e + \mathrm{i}\,d_e = \langle\alpha|\,\langle\beta|\phi_{ab}|\alpha\rangle\,|\beta\rangle = N_e \int_0^\infty v f\,(v)\,\mathrm{d}v \quad (3)$$
$$\times \left[\pi\rho_{\min}^2 + 2\pi \int_{\rho_{\min}}^{\rho_D} \rho \mathrm{d}\rho\,\langle\alpha|\,\langle\beta|S_a S_b^* - 1|\alpha\rangle\,|\beta\rangle\right],$$

where $f\,(v)$ is the Maxwellian electron velocity distribution function, ρ is the electron–radiator impact parameter, ρ_{min} — the smallest value of ρ below which the perturbation theory breaks down and S_a and S_b — the scattering matrixes of electrons–emitter collision corresponding to the initial and final state. In a regime of weak collisions, we calculate the width of the profile taking into account the contribution from the upper and lower level in the same manner, using the same order of perturbation theory. The data used for calculations of the matrix elements of the electric dipole moment and energy levels are determined based on the oscillator strengths and the atomic energy levels included in the NIST atomic spectra database [14] and Kurucz tables [17].

Besides calculations according to Griem's theory, we simulated profiles applying our numerical N-body code described in [5]. The advantage of the CSM is that it does not have any limitations, such as the cutting of the collision parameter for small values (i.e., the separation of the strong and weak collisions), the impact approximation for electrons and the quasi-static approximation for ions.

The plasma in this method is represented by a model of an ideal gas of the ions and electrons. The shape of the simulated volume is a sphere, with the electrically neutral emitter resting at its center. The radius of that sphere is equal to three Debye radiuses, because in distance $3r_D$ the shielding electric field is negligible.

In this work, the simulated profile results from taking into account the emission of about 500 emitters. Each individual radiation process is disturbed by the local electric fields produced by moving ions and electrons. The starting point of this consideration is the relation between the spectral line profile and the average of the dipole autocorrelation function

$$I(\Delta\omega) = \lim_{t_f\to\infty} \frac{1}{\pi} \int_0^{t_f} C(t)\, \mathrm{e}^{\mathrm{i}\,\Delta\omega t}\, \mathrm{d}t. \tag{4}$$

The average of the dipole autocorrelation function can be written in the following way:

$$C(t) = \mathrm{Tr}\left(\boldsymbol{d}_{if} \cdot U^{+}_{ff'}(t,0)\, \boldsymbol{d}_{f'i'} U_{i'i''}(t,0)\, \rho_{i''i} \right\}_{\mathrm{av}}, \tag{5}$$

where $U_{ii'}(t,0)$ and $U^{+}_{ff'}(t,0)$ are the time-evolution operators corresponding to the initial and final states while i, i' and f, f' indicate the sublevels of the initial E_i and final E_f states of the unperturbed atom, respectively. The frequency separation from the line center is given by $\Delta\omega = \omega - (E_i - E_f)/\hbar$. The averaging $\{\dots\}_{\mathrm{av}}$ is taken over all initial simulated field strengths and possible time histories.

For each local time history, the perturbation of the emitter structure is numerically calculated using the Schrödinger equation, satisfied by the time-evolution operators

$$\mathrm{i}\hbar\dot{U}(t,0) = (H_0 - \boldsymbol{d}\cdot\boldsymbol{F}(t))\, U(t,0), \tag{6}$$

where $\boldsymbol{d}$ is the dipole operator for the atom, $V(t) = -\boldsymbol{d}\cdot\boldsymbol{F}(t)$ is the radiator–plasma interaction potential and H_0 is the Hamiltonian of the isolated radiator. The Schrödinger equation describes an evolution of a quantum state of the emitter caused by electric fields varying in time, produced by ions and electrons. The equation is solved numerically, using the Strang symmetrical splitting formula. For details see [5, 18].

Figure 5 presents the comparison of the experimental $j(\lambda)$ profiles of the fine structure component $3p\ {}^4P^o_{2/5}$–$3d\ {}^4D_{3/5}$ obtained in the fitting procedure with a profile calculated according to the modified Griem theory and profile simulated using the CSM. As it can be observed, the simulated profiles and those calculated according to the Griem theory overlap. That means that the impact and quasi-static approximations work well in this case. The calculation results show that the contribution of ions to the line broadening is negligible.

We compared the calculated profiles with the experimental pure Stark $j(\lambda)$ profiles of the chosen spectral line, obtained using the fitting procedure. The asymmetry of the experimental profiles, as well as the FWHM is much larger than that of the calculated profiles. The difference between FWHM of the experimental $j(\lambda)$ profile and simulated profile can be analyzed, using the following quantity: $(\mathrm{FWHM}_{\mathrm{expt}} - \mathrm{FWHM}_{\mathrm{sim}})/\mathrm{FWHM}_{\mathrm{expt}}$. Its value,

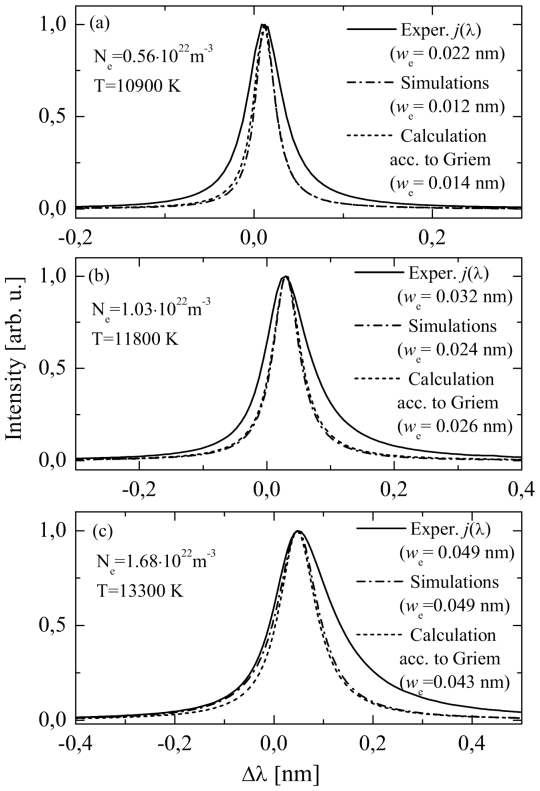

Fig. 5. The comparison of the experimental $j(\lambda)$ profiles of the spectral $3p\ {}^4P^o_{2/5}$–$3d\ {}^4D_{3/5}$ fine structure component at 1053.957 nm — results of the fitting procedure (solid lines), simulated profiles (dashed-dotted lines) and profiles calculated according to the modified Griem theory (short dashed lines) in three different plasma conditions.

in the cases shown in Fig. 5a, 5b and 5c, is respectively 44%, 40% and 30%. The difference between the calculated and measured profiles may indicate that the contribution of ions to the line broadening is underestimated in calculations or the model $j(\lambda)$ requires the inclusion of some additional factors, such as the quadrupole effect, quantum effects and backreaction effect. However, the determined electron impact widths of both experimental and theoretical profiles are quite similar, especially for higher electron densities. The relative difference between the experimental electron impact widths and the simulated ones, $(w_e^{\mathrm{expt}} - w_e^{\mathrm{sim}})/w_e^{\mathrm{expt}}$, is equal to 45%, 25% and 0%, corresponding to cases presented in Fig. 5a–c. According to the current state of the art, the best semiclassical perturbation methods provide the Stark impact widths which do not differ from the experimental data by more than 30% [19]. We do not reach this level only in the smallest electron densities.

6. Results

The comparison of electron impact widths determined experimentally, calculated using the computer simulation method and calculated using

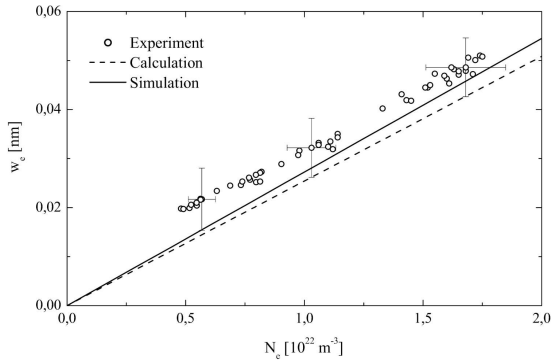

Fig. 6. The comparison of the electron impact widths w_e determined experimentally, using the fitting procedure (circles), calculated using the CSM (solid line) and calculated using the modified Griem theory (dashed line).

the modified Griem theory, is presented in Fig. 6. The electron impact width, as a function of the electron density, is shown.

The measured and calculated w_e are compatible with each other within uncertainty and the agreement is better at higher electron densities. The accuracy of the calculated Stark widths depends on the accuracy of the available atomic data. This type of uncertainty, which in the case of the studied multiplet indicates 50% accuracy, may explain discrepancies between the results of the simulation, calculation and experiment.

7. Summary and conclusions

The most important result of our work is that we obtained the consistent electronic Stark widths of the $3p\ ^4P^o$–$3d\ ^4D$ multiplet, using three different methods. Moreover, our results can be useful in determining electron density in low-temperature plasma. It is worth mentioning that the nitrogen multiplet lies in the near-infrared spectral range, poorly represented in the literature. Taking into account lower level contribution to the line shape in Griem's theory, the compatibility with the experiment improves by about 10%.

Our N-body simulation code extents the range of applicability of the CSM and allows to omit the impact and the quasi-static approximations but requires a very long calculation time.

References

[1] H.R. Griem, *Plasma Spectroscopy*, Mc Graw Hill, New York 1964.

[2] W. Lochte-Holtgreven, in: *Plasma Diagnostics*, Ed. W. Lochte-Holtegreven, Ch. 3, North-Holland, Amsterdam 1968.

[3] H.R. Griem, M. Baranger, A.C. Kolb, G. Oertel, *Phys. Rev.* **125**, 177 (1962).

[4] A. Bartecka, *Phys. Scr. T* **161**, 014065 (2014).

[5] K. Dzierżęga, Witold Zawadzki, F. Sobczuk et al., *J. Quantum. Spectrosc. Radiat. Transf.* **237**, 106635 (2019).

[6] J. Seidel, R. Stamm, *J. Quantum. Spectrosc. Radiat. Transf.* **27**, 499 (1982).

[7] T. Wujec, A. Bacławski, A. Golly, I. Książek, *Acta Phys. Pol A* **96**, 333 (1999).

[8] T. Wujec, W. Olchawa, J. Halenka, J. Musielok, *Phys. Rev. E* **66**, 066403 (2002).

[9] A. Bartecka, A. Bacławski, J. Musielok, *Cent. Eur. J. Phys.* **9**, 131 (2011).

[10] A. Bartecka, A Bacławski, J. Musielok, *J. Phys. B At. Mol. Opt. Phys.* **43**, 115004 (2010).

[11] M.A. Gigosos, V. Cardeñoso, *J. Phys. B* **29**, 4795 (1996).

[12] W.L. Wiese, D.E. Kelleher, V. Helbig, *Phys. Rev. A* **11**, 1854 (1975).

[13] F. Torres, M.A. Gigosos, S. Mar, *J. Quantum. Spectrosc. Radiat. Transf.* **31**, 266 (1984).

[14] A. Kramida, Y. Ralchenko, J. Reader et al., *NIST atomic spectra database (ver. 5.6.1)*, 2018.

[15] A. Bacławski, J. Musielok, *Spectrochim. Acta Part B* **65**, 113 (2010).

[16] J. Halenka, *Z. Phys. D At. Mol. Clust.* **16**, 1 (1990).

[17] R. Kurucz, B. Bell, *Atomic spectral line database from CD-ROM 23 of R.L. Kurucz*, Smithsonian Astrophysical Observatory, Cambridge 1995.

[18] G. Strang, *SIAM J. Numer. Anal.* **5**, 506 (1968).

[19] S. Sahal-Bréchot, M.S. Dimitrijević, N.B. Nessib, *Atoms* **2**, 225 (2014).